Austrian Journal of Earth Sciences | Volume 100 | 82 - 99 | Vienna | 2007

Multistratigraphy of the Draxllehen quarry near Berchtesgaden (Tuvalian – Lacian 2): implications for Hallstatt Limestone-sedimentation and palaeoclimate in the aftermath of the 'Carnian Crisis'.

Thomas HORNUNG

University of Innsbruck, Institute of Geology & Palaeontology, Innrain 52, 6020 Innsbruck, Austria
e-mail: tompal@gmx.net

KEYWORDS

Conodont biostratigraphy
Carnian-Norian boundary
Hallstatt limestone
Carbon isotopes
Oxygen isotopes
microfacies

Abstract

The Draxllehen quarry near Oberau/Berchtesgaden (central Northern Calcareous Alps) exposes a relatively thick, monotonously bedded Hallstatt red- and light-coloured limestone sequence. Detailed conodont biostratigraphy allowed for a concise age-dating of basal Tuvalian to Lower Norian including an approximate timeframe for the Carnian-Norian boundary (here defined by the first occurrence of *Norigondolella navicula*). This location represents one of the rare sites to study Hallstatt Limestone series deposited in the aftermath of the 'Carnian carbonate productivity crisis' thus documenting an immediate post-crisis re-insertion of carbonate precipitation. In addition, cross-correlation to isochronous sites and high variation in thicknesses of Hallstatt Red Limestones shed new light on the highly variable sedimentation onto 'Hallstatt deep swells'. Stages of different sediment accumulation triggered profoundly the depositional setting of Hallstatt Limestones and are recorded in the varying colour of carbonate rocks. Owing to very low CAI-indices of 1.0 and thus mild diagenetic alteration, this site was also suited for investigation of C- and O-stable isotopes of carbonate bulk samples. In the view of already existing Late Carnian isotopic data, the carbon trend highlights high Early Tuvalian $\delta^{13}C_{carb}$ ratios of 4.3 ‰ [V-PDB] steadily decreasing towards the Late Tuvalian. A minor positive shift of 0.4 ‰ around the Carnian-Norian boundary coincides to already known boundary sections. Supra-regional comparison, however, point to local effects rather than to globally important signals.

Eine relativ mächtige, monoton gebankte Hallstätter Rot- und Hellkalk-Abfolge wird aus dem Draxllehen-Steinbruch nahe Oberau/Berchtesgaden (zentrale Nördliche Kalkalpen) beschrieben. Altersmäßig wurde mit Conodonten basales Tuvalium bis unteres Norium belegt, sowie die Karnium-Norium Grenze mit Ersteinsetzen von *Norigondolella navicula* angenähert. Mit diesem stratigraphischen Spektrum stellt die hier vorgestellte Lokalität eine seltene Möglichkeit dar, eine weitgehend ungestörte, vollständige und überraschend mächtige Hallstätter Rotkalkfolge zu studieren, die direkt nach der sogenannten ‚Karnischen Krise' zur Ablagerung kam. Das impliziert nicht nur eine schnelle Erholung der Karbonatfabrik im Schelfbereich – biostratigraphische Korrelation zu benachbarten, wesentlich geringmächtigeren Rotkalkfolgen geben darüber hinaus neue Einblicke in das lokale Sedimentationsgeschehen an sogenannten ‚Hallstätter Tiefschwellen'. Die Ablagerungsgeschichte des Hallstätter Beckens wurde maßgeblich durch unterschiedliche Raten von Sedimentakkumulation auf Karbonat-Plattformen beeinflusst, womit sich die unterschiedliche Färbung der untersuchten Kalke in Einklang bringen lässt. Aufgrund geringer CAI-Indizes und einer vergleichsweise milden diagenetischen Überprägung eignet sich das vorliegende Profil weiters für Untersuchungen von stabilen Kohlenstoff- und Sauerstoff-Isotopen. Die aus Gesamtkarbonat gewonnen Daten stellen einen wichtigen Beitrag zur bislang spärlichen Datenbasis oberkarnischer Isotopenwerte und fügen sich gut in das bestehende Gesamtbild ein: den höchsten innerhalb der Trias gemessenen $\delta^{13}C_{carb}$-Signaturen von 4.3 ‰ [V-PDB] im Tuvalium 1 folgt ein beständiger Trend zu leichteren Werten. Ein positiver Exkurs nahe der Karnium-Norium Grenze dürfte jedoch – aus Vergleichen mit anderen Studien – eher lokalen Fraktionierungstrends denn überregionalen oder gar global bedeutsamen Isotopen-Signalen zuzurechnen sein.

1. Introduction

The lithological term "Draxllehen Limestones" is known since Schafhäutl (1851) and Gümbel (1861) and was put as representative for well bedded red limestones exhibiting a nodular texture of calcareous 'pseudoclasts' with chert intercalations. The type-locality, the small abandoned Draxllehen quarry near Oberau/Berchtesgaden, was studied consistently for more than one century (e.g. Schlosser, 1898; Plöchinger, 1955; Pichler, 1963; Donofrio, 1975). In the last decades, however, the name became unused since Pichler (1963) interpreted the carbonate rocks as a local (cherty) equivalent of the 'classic' Hallstatt Red Limestones Facies, known from many sites exposed in the central Northern Calcareous Alps. Ge nerally, Hallstatt Red Limestone-lithologies are to differentiate into a condensed non-nodular texture and a well bedded 'pseudoclastic'-cherty variation. Stratigraphically, they occur from Upper Ladinian to uppermost Carnian ('bedded red limestones'

or 'nodular red flaser limestones' in Mandl, 2000) and in the Upper Norian ('Hangendrotkalk' in Schlager, 1969; 'upper red limestones' in Mandl, 2000). Their presence is associated with so-called 'Hallstatt deep swells': induced by halokinetic movements of 'Permoskythian Haselgebirge' on instable deep shelf regions (e.g. Schlager, 1969; Tollmann, 1976; Brandner, 1978), these synsedimentary ridges are thought to have influenced highly variable sedimentary patterns (Mandl, 1984, 2000).

In recent years, almost all Hallstatt Limestones outcrops around Bad Dürrnberg and Oberau/Berchtesgaden have been studied by lithologic, microfacies and biostratigraphic points of view (e.g. Gawlick and Lein, 1997, 2000; Gawlick et al., 1999, Gawlick, 2000; Hornung and Brandner, 2005; Hornung, 2005, 2006a, 2006b; Hornung et al., 2007b). Their variance of thickness – 0.5-3.0 m for the Tuvalian at the Feuerkogel near Bad Aussee (Salzkammergut; see Krystyn, 1991) and 80-100 m for the Tiefenbachgraben succession near Marktschellenberg/Berchtesgaden (Plöchinger, 1955; Pichler, 1963) – implies two possibilities: a) narrow variations in primary sediment accumulation or b) postsedimentary variations due to tectonic duplication or tripling (e.g. Gawlick et al., 2001; Missoni, 2003). Both phenomena can be confirmed or disproved only by detailed biostratigraphic investigations.

The Draxllehen succession is dissected by several flat normal faults (Figs. 2a-b); however, detailed conodont biostratigraphy allowed for reconstruction of the original thickness (circa 25 m) that encompasses the complete Tuvalian (Upper Carnian) and the basal Lacian (Lower Norian). Accordingly, the Draxllehen outcrop is one of the rare exemptions that expose Hallstatt Red Limestones of Tuvalian 1 age and document thus basinal carbonate deposition in the immediate aftermath of the siliciclastic 'Carnian Event' that affected nearly all marginal Tethyan facies areas (e.g. Hallam, 1996; Lehrmann et al., 2005; Hornung et al., 2007a) and documents both a major demise of reefs and a significant carbonate productivity crisis, followed by a major change in the diversity of carbonate producers a few million years later (Flügel, 2002). In addition, the aforementioned relative high thickness of Draxllehen Hallstatt Red Limestones plays a crucial role in understanding Hallstatt Limestone-deposition onto highly mobile 'Hallstatt deep swells' (e.g. Schlager, 1969; Reading, 1986; Mandl, 1984, 2000).

Owing to good accessibility and exposure, excellent biostratigraphic control and mild late diagenetic alteration, the Draxllehen succession is also suited for isotope investigations on carbonate whole rocks that provide new constraints to the sparse database of Late Triassic whole rock isotope values (Steuber, 1989; Lintnerova and Hladikova, 1992; Bellanca et al., 1995; Gawlick and Böhm, 2000; Hornung and Brandner, 2005; Korte et al., 2005).

2. Geological setting

The studied section is located at the eastern wall of the Draxllehen quarry near Oberau (5 km NE of Berchtesgaden;

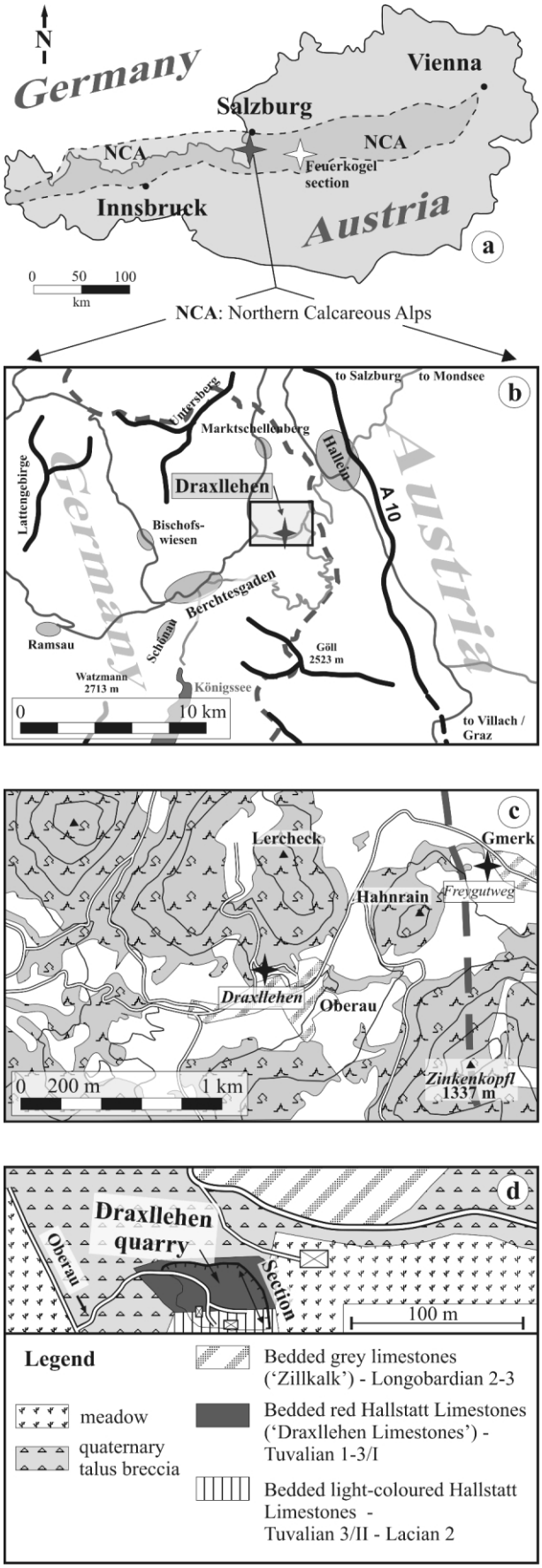

Figure 1: (a, b) Geographic overviews. (c) Location of the Draxllehen succession and the Freygutweg (in Gawlick et al., 1999a; Hornung and Brandner, 2005). (d) Simplified geological map of the area around the Draxllehen quarry.

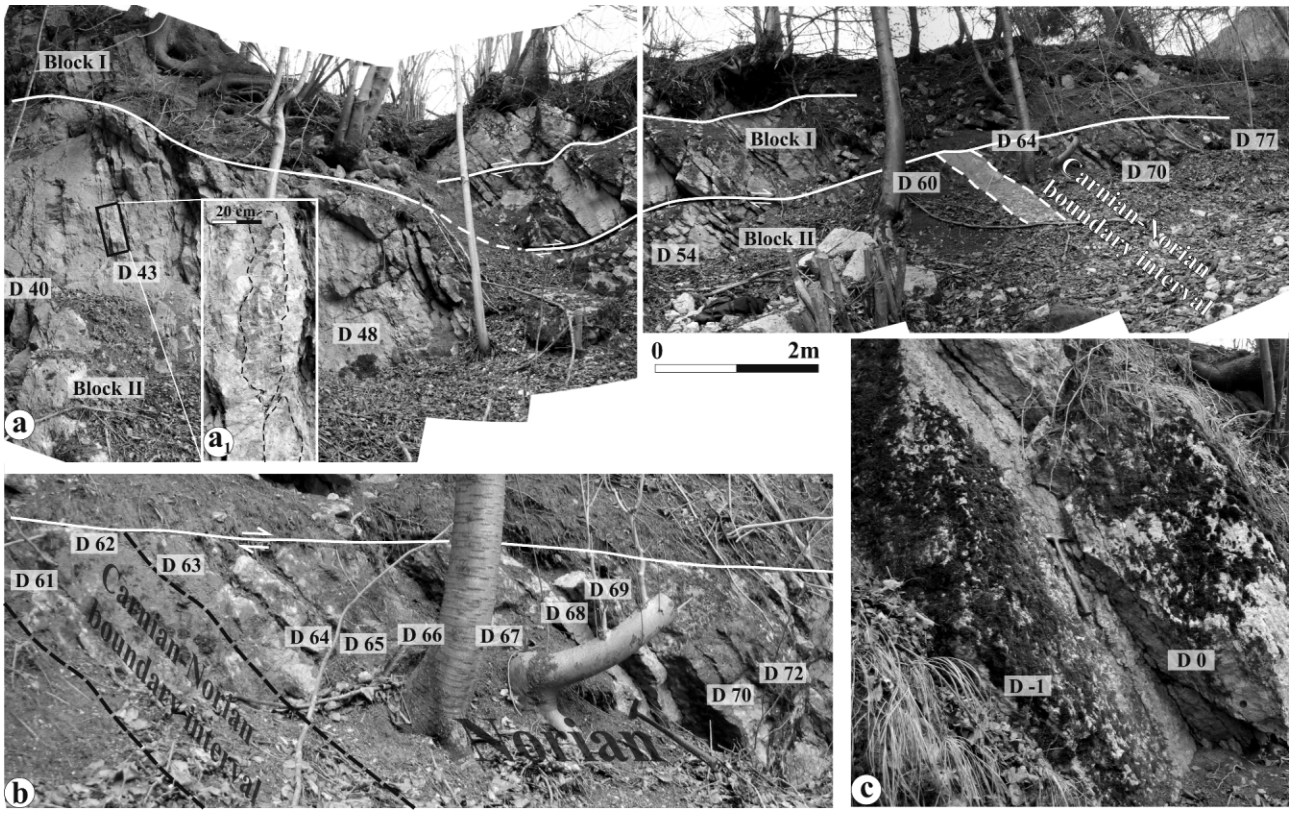

Figure 2: (a) The upper part of the Draxllehen succession (situation in January 2007) with some sampling points / horizons and the approximated position of the Carnian-Norian boundary. (a1) Detail from horizon D 43 highlighting a magenta-coloured chert-nodule. (b) Detail from the approximated Carnian-Norian boundary (hammer to scale). (c) The lowermost part of the studied sequence exposes grey-coloured limestones with a reddish hue (hammer to scale).

UTM: WGS84, Zone 33; E 354772; N 5279684; Figs. 1a-d; for the name of the quarry see also Rieche, 1971) and exposes, from bottom to top, well-bedded greyish-red-, magenta-red- and light-coloured limestones (Figs. 2a-c). All beds dip uniformly to SSW at 57°-65°. The section is crossed by flatly dipping normal faults (240/15), which dismember the succession into two blocks (Figs. 2a-b, 4).

The Upper Carnian to Lower Norian Hallstatt limestones of the Draxllehen succession are part of the 'Hallein-Berchtesgadener Hallstätter Schollenregion', a tectonic unit that is characterised by a chain of displaced nappe sheets ('Lower Juvavic Nappe' in Gawlick and Böhm, 2000) squeezed between the Tirolic Nappe below and the Berchtesgaden Nappe above ('Upper Juvavic Nappe' in Gawlick and Böhm, 2000; see also Pichler, 1963; Zankl, 1971; Tollmann, 1976; Decker et al., 1987; Frank, 1987; Langenscheidt, 1994). Tectonic framework, i.e. concepts about mechanism and timing of block emplacement are still matter of a vivid discussion (Frisch and Gawlick, 2003, cum. lit.).

3. Material and methods

52 samples were collected from in situ beds of the Draxllehen quarry in spring 2006 and winter 2007. In addition, carbonate hand specimens and thin-sections of Donofrio (1975), R. Brandner and W. Mostler (all Innsbruck; field work in summer 1992), were re-investigated. All samples have been treated with acetic acid; conodont material and microfauna were extracted from the insoluble residues (archive Institute of Geology and Paleontology, University of Innsbruck, Hornung, 'Draxllehen': D -2 – D 77). The CAI (Conodont Colour Alteration Index) of every conodont was determined according to Epstein et al. (1977) and Jones (1992). Taxonomy and classifications of conodonts are based mainly on the studies of Krystyn (1980, 1983; see also synonymy list at the conodont

Figure 3: Microfacies of the Draxllehen quarry: (a) Filament- and crinoid packstones, overprinted by pressure solution causing a 'pseudoclastic' texture ('psk'; bed D 8). Note the amputation of the spar-filled fissure by a stylolithes (black arrow). (b) The primary microstructure of biograins have been preserved despite of silicification (b_1: brachialia and b_2: centrodorsalia of *Osteocrinus* sp.). The carbonatic matrix, here dark grey-coloured, consists of fused peloids (D 11). (c, d) Filament packstones (D 8) compared to radiolarian wackestones (D 14). Note the halobiid shell (white arrow), the calcified radiolarians (white oval) and ostracod shells ('umbrella porosity' and geopetal fabric, black arrow). (e) Biogenous wackestone grading into a poorly sorted lithoclastic packstone (D 15). Note the marginal bioerosion of lithoclasts (black arrows). (e_1) Loosely packed matrix consisting of fused peloids and ostracod shells. (e_2) Angular section through a textulariid foraminifer. (e_3) Siliceous sponge spicule. (f) Breccia 2 (D 18) is characterised by angular, poorly sorted lithoclasts surrounded by a dense micritic matrix. The two white ovals highlight grains encrusted by syntaxial cement seams, the white arrows point to lithoclasts with spar-filled fissures indicating early cementation prior to sediment reworking and thus low sediment accumulation rates. (g) Filament packstone consisting mainly of halobiid shell debris (D 19). (h) The bright-coloured limestones of 'part III' contrasts by their monotonous radiolarian fauna associated with rare filaments and juvenile ammonoid fragments (white arrow) (D 72).

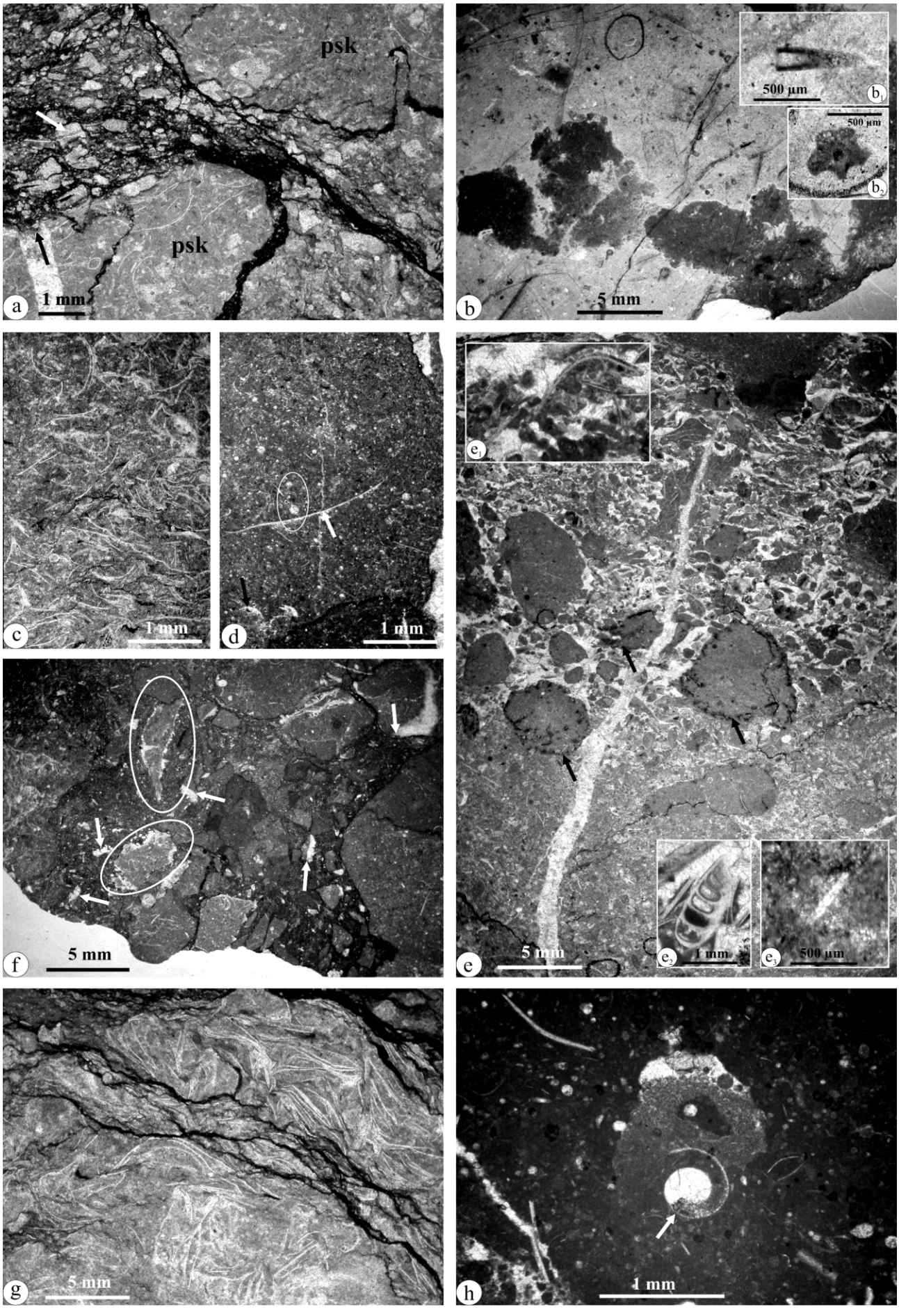
psk
psk
1 mm
a
500 µm
b1
500 µm
b2
5 mm
b
1 mm
c
1 mm
d
e1
5 mm
e
1 mm
e2
500 µm
e3
5 mm
f
5 mm
g
1 mm
h

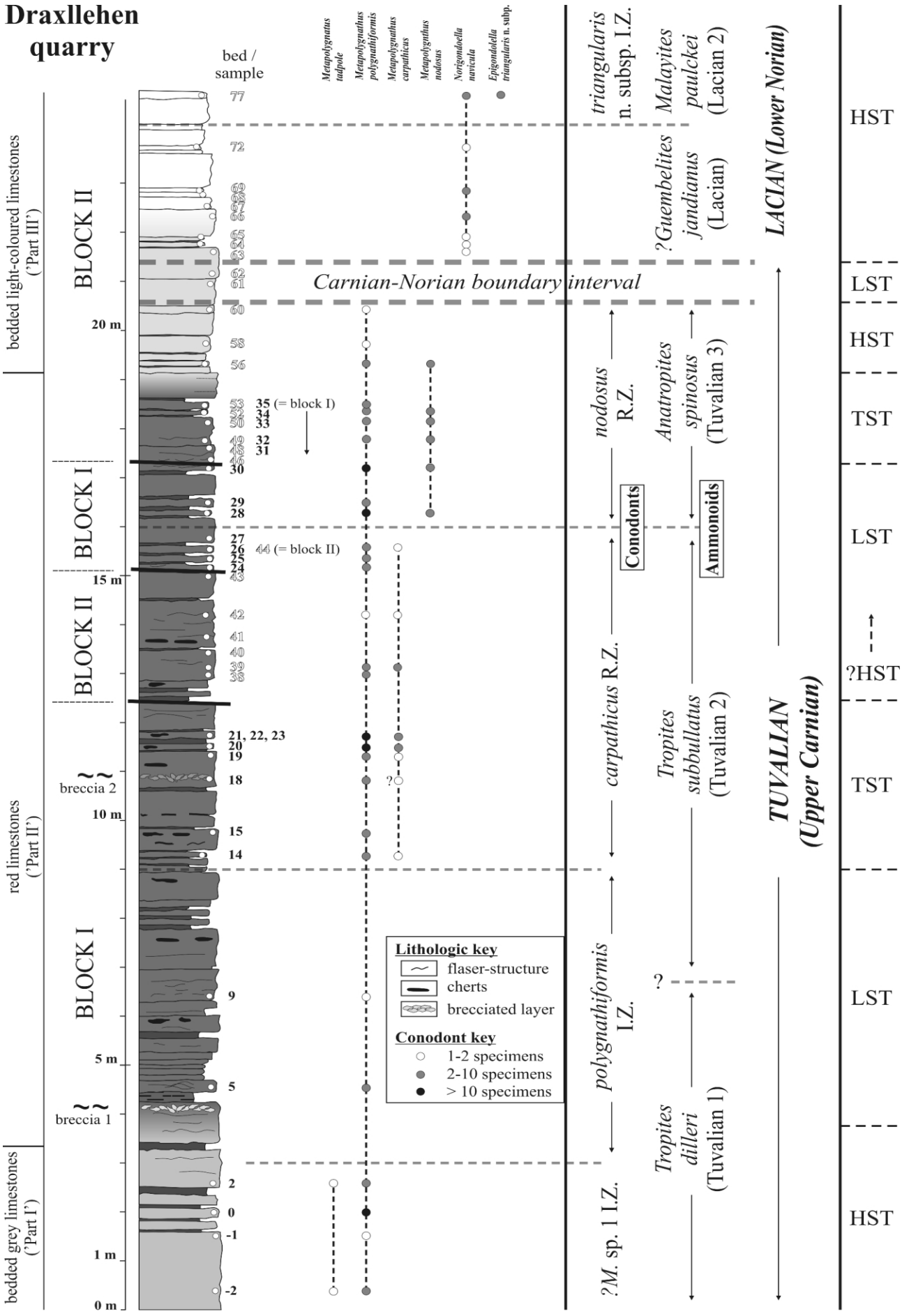
Draxllehen quarry
bed / sample
Metapolygnatus tadpole
Metapolygnatus polygnathiformis
Metapolygnatus carpathicus
Metapolygnatus nodosus
Norigondolella navicula
Epigondolella triangularis n. subsp.
bedded light-coloured limestones ('Part III')
red limestones ('Part II')
bedded grey limestones ('Part I')
BLOCK II
BLOCK I
BLOCK II
BLOCK I
breccia 2
breccia 1
20 m
15 m
10 m
5 m
1 m
0 m
77
72
60
58
56
35 (= block I)
34
33
32
31
30
29
28
27
26
25
24
44 (= block II)
43
42
41
40
39
38
21, 22, 23
20
19
18
15
14
9
5
2
0
-1
-2
Carnian-Norian boundary interval
Lithologic key
flaser-structure
cherts
brecciated layer
Conodont key
1-2 specimens
2-10 specimens
> 10 specimens
triangularis n. subsp. I.Z.
nodosus R.Z.
carpathicus R.Z.
polygnathiformis I.Z.
?M. sp. 1 I.Z.
?Guembelites jandianus (Lacian)
Malayites paulckei (Lacian 2)
Anatropites spinosus (Tuvalian 3)
Tropites subbullatus (Tuvalian 2)
Tropites dilleri (Tuvalian 1)
Conodonts
Ammonoids
LACIAN (Lower Norian)
TUVALIAN (Upper Carnian)
HST
LST
HST
TST
LST
?HST
TST
LST
HST

description). The biostratigraphic interpretations follow Krystyn (1978), Gallet et al. (1994) and Krystyn and Gallet (2002), although other Late Carnian and Early Norian biozonation-models are in parallel use (Orchard, 1991a, b; Kozur, 2003). The former authors are preferred because their considerations are based on investigations that were done predominantly in the alpine-mediterranean facies domain, but have been proved even in far-distanced Tethyan regions (Turkey, SW' Tethys: e.g. Gallet et al., 1994; 1996, 2003; Krystyn et al., 2002; Krystyn and Gallet, 2002; Spiti, S' Tethys: Garzanti et al., 1995; Bhargava et al., 2004; Timor, SE' Tethys: Martini et al., 2000).

Oxygen and carbon stable isotope ratios were measured in all calcareous and marly beds. Four whole-rock powder samples (0.05-0.37 mg) were bored with a dental drill from fresh surfaces. Attention was paid in drilling only homogenous mudstones and small bioclasts, and not cement-filled bioclasts and/or fissures and not pressure solution seams. The powders reacted in 10 ml borosilicate extainers with phosphoric acid after flushing with He. Generated CO_2 was separated from water vapour and was analysed for $\delta^{13}C_{carb}$ and $\delta^{18}O_{carb}$ on a Gas Bench II linked to a ThermoFinnigan Delta^{plus} XL mass spectrometer (Spötl and Vennemann, 2003). The results were calibrated against VPDB (Vienna Pee Dee Belemnite). The aimed reproducibility of isotopes values is ± 0.06 ‰ (1σ) for $\delta^{13}C_{carb}$ and ± 0.08 ‰ (1σ) for $\delta^{18}O_{carb}$.

4. Results

4.1 Microfacies

The Draxllehen quarry succession starts with dm-bedded grey limestones (thickness circa 5 m, samples D -2 – D 2: part I), overlain by dm-bedded red limestones with chert nodules (thickness circa 18 m; samples D 5 – D 56; part II) and bedded light-coloured limestones (thickness 7 m; samples D 58 – D 77; part III).

The bedded grey limestons ('part I') are filament packstones. The fine micritic matrix yields abundant, chaotically aligned filaments *(Halobia* sp.), sphaerical calcified radiolarians, ostracods and rare dense micritic (?algal) microproblematica. The primary depositional lamination has been destroyed by homogenous burrowing. The grey limestones are confined by a distinct breccia (sample D 4). The overlying dm-bedded red limestones are burrowed filament-bearing bioclastic wackestones and radiolarian wackestones and packstones. From samples D 5 to D 14, the abundance of filaments decreased at the expense of more common radiolarians (Figs. 3c-d). Here, the most common biograins are – next to filaments and sphaerical calcified radiolarians – planktonic crinoids (brachialia and centrodorsalia of *Osteocrinus* sp.), small turritelliticon gastropods, rare ostracod shell debris, textulariid foraminifers (Fig. 3e$_2$) and calcified sponge spiculae (Fig. 3e$_3$). Some subangular lithoclasts observed in a winnowed, crinoid-bearing bioclastic grainstone texture are bored by endolithic worms (D 15, see Fig. 3e) and comparable to the variety 'Gewundene Gänge' of Schmidt (1990:114). Further bioturbation can be noticed by distinct burrows and their loosely packed micritic infill.

The second brecciate layer (sample D 18) exhibits a chaotic, component-supported fabric consisting of angular lithoclasts (radiolarian wackestones of underlying horizons; D 14 – Fig. 3f). Some of the lithoclasts are surrounded by isopachous calcite cement seams. Amputation of some sparfilled fissures within lithoclasts infers brecciation after lithification (Fig. 3f).

Within the horizons D 19 to D 56, the microfacies patterns are quite similar to the above described development: filament packstones, as shown in Figure 3g, grade into radiolarian wackestones. Above D 56, the red colour of the limestones give way into a pink- and finally into a light-coloured hue (above D 66). Being nearly pure burrowed radiolarian wackestones with a fine, dense micritic matrix, the sole accessorial biograins are thin-shelled ostracods, filaments (halobiids or ammonoid shells) and embryonal ammonoids (Fig. 3h).

4.2 Diagenesis

4.2.1 Conodont Colour Alteration Index (CAI)

All investigated conodont material derives from 39 different samples with CAI-values of 1.0. According to Epstein et al. (1977) and Jones (1992), this represents an upper limit of 50-80°C during burial diagenesis and coincides well to the Berchtesgaden CAI-provenance of Gawlick and Königshof (1993) and Gawlick et al. (1994), and, in addition, well to the temperature estimates of Rieche (1971:154), which are based on clay mineral groups and range between minimum values of 30°C and maximum degrees of 80°C. Accordingly, a significant diagenetic overprint in deep burial stages can be neglected a priori, and proves the Draxllehen succession as suitable for isotope investigations on carbonate whole rocks.

4.2.2 Cements and microtectonic

One main characteristic of the Draxllehen succession is the intensive pressure solution that created – by the combination of vertical and horizontal stress components – a nodular, 'pseudoclastic' texture (Fig. 3a). That pressure solution happened at deeper burial levels and is obvious if viewing at spar-cemented tension fissures, which are cut by stylolithe

Figure 4: Lithological chart and conodont biostratigraphy of the Draxllehen succession. The differentiation in 'block I' and 'block II' refers to the tectonically overprinted sequence – the position of the normal fault is emphasized by the black bold lines. The conodont and ammonoid biozonation follow Gallet et al. (1994) and Krystyn and Gallet (2002). Abbreviations: I.Z. = conodont interval zone; R.Z. = conodont range zone. The sequence-stratigraphic interpretation on Tuvalian / Lower Lacian carbonate platforms follows Krystyn and Lein (1996). Abbreviations: HST = highstand system tract; TST = transgressive system tract; LST = lowstand system tract.

seams (Fig. 3a). The second characteristic of the studied sequence is the partial silification of the texture (Fig. 3b), with preservation of primary bioclastic structures (Figs. $3b_1$-b_2). Even here, the metasomatosis took place during deep burial and derived from siliceous fluids. Chert-intercalations are most common in the lower part of the section and disappear above bed D 43 (Figs. 2a-b).

4.2.3 X-Ray diffractometry

The potential dolomite content of all measured Draxllehen carbonate rocks were below the detection limit (i.e. more than 1 %). All measured samples are composed nearly exclusively of calcite – sample D -2 contains accessorial quartz (ca. 2 %).

4.3 Biostratigraphy

This chapter includes only descriptions of conodonts, which are important for biozonation (in order of their first stratigraphical appearance). Not described is the species *Metapolygnathus polygnathiformis* (D -2 to D 60, see Figure 4 and plate 1, Fig. b), a long-ranging Carnian species. Not described and figured are *Paragondolella* cf. *lindae* (D 48), *Metapolygnathus pseudoechinatus* (D 58), questionable juvenile (and thus not biostratigraphically considered) *Epigondolella* cf. *primitia* (D 69, D 72) and *Epigondolella* ex gr. *abneptis* (sensu Orchard, 1983; D 63; D 64, D 65; D 66, D 69)

Metapolygnatus tadpole (Hayashi, 1968)

1968 *Gondolella tadpole* n. sp.; in Hayashi (1968): pl. 1, fig. 6
1972 *Gondolella tadpole* (Hayashi, 1968); in Kozur (1972): pl. 3, figs. 7-8
1980 *Gondolella tadpole* (Hayashi, 1968); in Kovacs and Kozur (1980): pl. 9, figs. 4-5
1983 *Gondolella tadpole* (Hayashi, 1968); in Kovacs (1983): pl. 2, figs. 3-4
Pl. 1, Figs. 1a1, a2
Material: Rare occurrence in D -2 and D 2 (two specimens).
Description: Characteristics are the short and slightly reduced platform that extends posteriorly after midlength and the elongate free blade, which consists of highly fused carinal teeth. The even carina is highest in midlength and descends slightly towards anterior. The considerably stronger developed two terminal teeth are stepped and declined posteriorly with respect to the basal keel. Unlike to the arched *Metapolygnathus polygnathiformis*, this unit is not arcuated. The honeycomb structure extends to the whole platform. The posterior basal keel is broad and oval-shaped and includes a very narrow basal pit.
Remarks: As discussed in Krystyn (1983:241), *M. tadpole* is synonymous to *Paragondolella foliata foliata* (sensu Kovács, 1983). *Metapolygnthus* n. sp. 1 (sensu Krystyn, 1983) differs from *M. tadpole* by its more reduced platform and longer free blade (Krystyn, 1983, and L. Krystyn, pers. comm. 2007).
Stratigraphical occurrence: Longobardian - Tuvalian 1/I (Krystyn, 1983, and pers. comm. 2007).

Metapolygnathus carpathicus (Mock, 1979)

1979 *Gondolella carpathica* n. sp.; in Mock (1979): pl. 1, figs. 1-5
1980 *Gondolella carpathica* Mock (1979); in Kovács and Kozur (1980): pl. 10, fig. 5 (non 6)
1983 *Epigondolella nodosa carpathica* (Mock, 1979); in Kolar-Jurkovsek (1983): pl. 24, figs. 5a-b
2003 *Paragondolella carpathica* (Mock, 1979); in Channell et al. (2003): pl. 1, figs. 4, 5, 7, 9, 10
Pl. 1, Figs. c1, c2
Material: Frequent from D 14 to D 44 (ca. 20 specimens)
Description: *M. carpathicus* evolved from *M. polygnathiformis* (Mock, 1979). Affinities exist a) in the subquadrate, anteriorly rapid declining platform that encompasses the complete, posteriorly arched unit, b) in a low carina consisting of fused older teeth, c) in the microreticulation and d) the bulged platform rims. The main difference with respect to *M. polygnathiformis* can be seen in two to three distinct marginal nodules at the declining anterior part of the platform. These teeth may alter posteriorly in roundish nodules similar to *M. nodosus*. The carina ascends consistently towards anterior. The keel is branched posteriorly and embraces a narrow basal pit.
Stratigraphical occurrence: *carpathicus* conodont interval zone (= upper *subbullatus* ammonoid Zone or Tuvalian 2/II; see Figure 4).

Metapolygnathus nodosus (Hayashi, 1968)

1968 *Gladigondolella abneptis* var. *nodosa* var. nov.; in Hayashi (1968), pl. 2, figs. 9a-c
1973 *Epigondolella nodosa* (Hayashi, 1968); in Krystyn (1973): pl. 3, figs. 2-4
1980 *Gondolella nodosa*, Hayashi (1968); in Krystyn (1980): pl. 12, figs. 1-7
1980 *Metapolygnathus nodosus* (Hayashi, 1968); in Kovács and Kozur (1980): pl. 12, figs. 1-4
1991 *Metapolygnathus nodosus* (Hayashi, 1968); in Orchard (1991a): pl. 2, figs. 8-13
2003 *Epigondolella nodosus* (Hayashi, 1968); in Channell et al. (2003): pl. 1; figs. 14, 19-21, 23, 28, 30-33
Pl. 1, Figs. d1, d2
Material: Common occurrence from D 28 to D 56 (10 specimens).
Description: Orchard (1991a) described this species by highly variable platform ornamentation: the main characteristic is the development of several indistinct marginal nodules, which start at the anteriorly declining platform and proceed towards posterior. This is different to *M. carpathicus*, whose nodes in midlength are more distinct and whose posterior platform is

scupltureless. The slightly arched platform spreads over one half to two third of the unit declining towards the anterior free blade. The carina consists of highly fused denticles and ascends consistently towards anterior.

Stratigraphical occurrence: *nodosus* conodont I.Z. (= *spinosus* ammonoid Zone or Tuvalian 3; see Figure 4).

Norigondolella navicula (Huckriede, 1958)

1958 *Gondolella navicula*, n. sp.; in Huckriede (1958): pl. 11, figs. 1-4, 13-19, 27, 35; pl. 12, figs. 2-8, 10, 15-22, 24-27

1980 *Gondolella navicula*, Huckriede (1958); in Krystyn (1980): pl. 11, figs. 10-11

1983 *Gondolella navicula*, Huckriede (1958); in Kolar-Jurkovsek (1983): pl. 4, figs. 1a-c

1991 *'Neogondolella' navicula* (Huckriede, 1958); in Orchard (1991a): pl. 4, fig. 13

2003 Norigondolella navicula (Huckriede, 1958); in Channell et al.(2003): pl. 2; figs. 7-10, 12, 13, 15, 21, 34, 35; pl. 3, fig. 11

Pl. 1, Figs. e1, e2

Material: Common occurrence from D 63 to D 77 (17 specimens).

Description: Large, slightly arched and slender units with a strongly developed stepped terminal nodule, followed by a protracted ridge with older teeth. The thickly bulged platform rim surrounds the posterior denticle from its earliest introduction. The clear microreticulation covers the complete platform except the adcarinal troughs. The posteriorly circular widened keel embraces a terminal basal pit.

Stratigraphical occurrence: Lacian 1 – Sevatian 2 (Krystyn, 1980).

Epigondolella triangularis n. subsp. (sensu Krystyn and Gallet, 2002)

1972 *Ancryogondolella triangularis* n. gen. n. sp.; in Budurov (1972): pl. 1, figs. 3-6

2003 *Epigondolella trianguaris* (Budurov, 1972); in Channell et al.(2003): pl. 3; fig. 19

Pl. 1, Figs. f1, f2, g1, g2

Material: Exclusive occurrence in horizon D 77 (4 specimens)

Description: Strongly ornate epigondolellid conodont with an assymmetrical trapezoidal to triangular posterior platform. Three to four distinct and upright denticles encircle the anterior platform margins; nodes on posterior brims are developed less discrete and may merge diagonally into indistinctive secondary carinas. The blade has developed 11 to 12 denticles and a stepped posterior nodule that is asymmetrically displaced before a central constriction or a nodule at the terminal platform brim. Commonly, the carinal denticles are highest in midlength. The bifurcated basal scar wears a subcentral situated pit.

Remarks: *E. triangularis* n. subsp. differs from *E. abneptis* A (sensu Krystyn and Gallet, 2002:14) by its asymmetrical

Sample	$^{13}C_{carb}$	$^{18}O_{carb}$
D 1	4,21	-0,63
D 2	4,14	-0,94
D 3	4,15	-0,76
D 4	4,07	-0,49
D 5	3,9	-0,56
D 6	3,71	-0,71
D 7	3,83	-0,73
D 8	3,8	-1,23
DD 9	3,81	-1,34
D 10	3,81	-0,88
D 11	3,78	-0,73
D 12	3,69	-0,59
D 19	3,65	-0,71
D 20	3,67	-0,85
D 22	3,69	-0,75
D 24	3,49	-1,04
D 25	3,45	-0,65
D 27	3,47	-0,8
D 28	3,25	-0,79
D 29	3,5	-0,31
D 30	3,44	-0,72
D 31	3,51	-0,85
D 32	3,45	-0,58
D 33	3,41	-0,83
D 34	3,46	-0,3
D 35	3,46	-0,2
D 36	3,52	-0,73
D 37	3,69	-0,32
D 39	3,36	-0,51
D 40	3,28	-0,82
D 41	3,45	-0,29
D 42	3,5	0,35
D 43	3,5	-0,71
D 44	3,44	-0,63
D 45	3,25	-0,59
D 46	3,3	-1,23
D 47	3,42	-0,48
D 48	3,32	-0,8
D 49	3,4	-0,67
D 50	3,36	-0,59
D 52	3,35	-0,64
D 53	3,18	-0,75
D 56	3,5	-0,35
D 60	3,31	-1,4
D 61	3,74	-0,9
D 63	3,72	-0,8
D 64	3,59	-0,62
D 65	3,75	-1,16
D 67	3,5	-1,02
D 68	3,615	-0,7
D 69	3,45	-0,83
D 72	3,4	-0,63
D 77	3,33	-0,66

TABLE 1: Carbon and oxygen isotopes of measured samples.

posterior platform, from *E. triangularis* s. str. (Budurov and Stefanov) by smaller platform nodes and 'a less widening posterior platform'.

4.3.1 Biozonation

According to Krystyn (1983) and Gallet et al. (1994), *M. tadpole* occurs from the Late Ladinian (Longobardian) and Early Carnian, whereas the genus *Gladigondolella* disappears at the top of the Early Carnian. Recent studies (Gawlick et al., 1999; Bhargava et al. 2004; unpubl. data Leo Krystyn, Vienna), however, proved this species also within the Early Tuvalian. Hence, *M. tadpole* without *Gladigondolella* evidences the Tuvalian 1 (= *Metapolygnathus* sp. 1- interval zone [I.Z.] or the lower *dilleri* ammonoid Zone) in the Draxllehen quarry, at least within the bedded grey limestones from samples D -2 to D 2 ('part I').

Above, the monospecific occurrence of *M. polygnathiformis* without other conodont species (e.g. the long-ranging genus *Gladigondolella*; compare to Krystyn, 1980), assign the *polygnathiformis* I.Z. (samples D 5-D 13; Tuvalian 1/II-2/I; upper *dilleri-* to lower subbullatus ammonoid Zone). The first occurrence of *M. carpathicus* in D 14 defines the base of the *carpathicus* range zone (abbr: R.Z.; Tuvalian 2/II; upper *subbullatus* ammonoid Zone), the FO of *M. nodosus* in D 28 the base of the nodosus R.Z (*spinosus* ammonoid Zone or Tuvalian 3). The latest Tuvalian conodont zone, defined by the species *Metapolygnathus communisti* A (Tuvalian 3/II sensu Krystyn, 1980), was not observed at Draxllehen. This might be due to the comparatively meagre Draxllehen conodont fauna (relative to the Freygutweg or Feuerkogel fauna), or indicate a short stratigraphic hiatus in the latest Tuvalian. A tectonic reduction induced by the flat normal faults can be definitely excluded (see Figure 4).

The FO of *N. navicula* in horizon D 63 is important for the biozonation of the Draxllehen quarry, as the ammonoid Carnian/Norian boundary (*spinosus* / *jandianus* Zone) is here arbitrarily approximated with the first appearance datum (FAD) of this species (compare to Krystyn, 1980, and Rigo et al., 2007). Current studies, however, highlight the different FAD of *N. navicula* 'from one area to another' (Krystyn and Gallet, 2002:12) and as facies-controlled (Kozur, 2003), pointing to the unsatisfactory biostratigraphic significance of this species. The now favoured *Metapolygnathus communisti* B (Lacian 1/I) was not found in the Draxllehen succession, indicating that the stratigraphical hiatus may encompass the earliest Lacian, too. *Metapolygnathus abneptis*, the index species of the Lacian 1/II, was found but is not figured due to uncertain determination of exclusively juvenile growth stages.

The FAD of Epigondolella triangularis n. subsp. in D 77 defines the Lacian 2/I-II (Lower jandianus ammonoid Zone; L. Krystyn, pers. comm. 2007).

4.4 Stable isotopes

The $\delta^{13}C_{carb}$-data show a regressive trend from 4.3 ‰ (V-PDB) in D 1 to 3.2 ‰ in D 77 (Fig. 5a). Most prominent is a minor positive shift of 0.4 ‰ between D 60 and D 61 within the approximated Carnian-Norian boundary interval.

Oxygen isotope values ($\delta^{18}O_{carb}$) range between -0.3 ‰ (V-PDB) in D 41 and -1.4 ‰ in horizon D 60. Taken 0.5 ‰ as 'background value', five indistinct negative shifts can be noticed: in D 9 (I), D 40 (II), D 24 (III), D 48 (IV) and D 60 (V). All values are listed in Tab. 1.

5. Discussion

5.1 Facies development

5.1.1 The Draxllehen depositional area

The Draxllehen Hallstatt Red Limestone succession, being part of the 'varicoloured' Hallstatt Facies of the Salzkammergut (Mandl, 2000), document sedimentation in a distal, open-marine periplatform setting on NW' Tethyan margins located at the transition zone to the 'Hallstatt-Meliata Ocean' (Kozur and Mostler, 1992; Mandl and Ondrejikova, 1993; Gawlick, 1993; Channel and Kozur, 1997).

In the Upper Triassic, the evolution of calcareous planktonic nannofossils was still in evolutionary progress (e.g. Bralower et al., 1991; Janofske, 1992; Bellanca et al., 1995). Hence, Tuvalian calcareous plankton is thought to have contributed only minor parts to limestone sedimentation in eupelagic settings. The primary source areas of all carbonate lime were thus shallow-marine carbonate platforms in close adjacency (e.g. Early Carnian: Wetterstein Platform; Norian: Dachstein Platform, see Gawlick and Böhm, 2000). Accordingly, the Hallstatt Limestones exposed at Draxllehen show only unimportant amounts of biogenous shells, i.e. silica- and carbonate-walled biota, which contributed to limestone sedimentation as 'allochthonous' pelagic rain and/or as 'autochthounous' benthos: the former are mainly pseudoplanktonic, thinshelled halobiids (i.e. 'filaments'), planktonic crinoids, spherical, primary siliceous radiolarians and phosphatic jaws of presumably nektonic, enigmatic conodontophorids, the latter are ostracods

Figure 5: Isotope stratigraphy of: (a) the Draxllehen quarry; (b) the Dürrnberg section ('Freygutweg' and 'Jakobberg gallery'; Hornung and Brandner, 2005; Hornung, 2006a) and (c) the Feuerkogel (Krystyn, 1973, 1980, 1991). Insert (1) illustrates the presumed palaeogeographic situation in the Late Tuvalian (modified after Haas et al., 1995): Wetterstein Carbonate Platforms are covered by a mixed siliciclastic-evaporitic-carbonatic succession ('Raibl-Opponitz' platform) that extended towards the Hallstatt Basin and 'Hallstatt deep swells' (Hds), on which the position of the successions (a-c) is estimated. (2) Schematic and exaggerated NW-SE cross-section following the dashed black line of (1): Wetterstein Carbonate Platforms and intraplatform basinal troughs ('Reifling Basin') had been refilled by Reingraben Shales and the siliciclastic Lunz Formation (s.str.), finally covered by limestones of the 'Northern Alpine Raibl'- and Opponitz Formations (W' and E' NCA, respectively), prograding towards the oceanic-related Hallstatt Basin. (3) Detail from the 'Hallstatt deep swell' bearing the Hallstatt Red Limestone-Facies: synsedimentary halokinetic movements generated local up- and downlift-structures with differing rates of tectonic subsidence and, accordingly, different thicknesses of Hallstatt Red Limestones (note the positions of the sites a, b, and c).

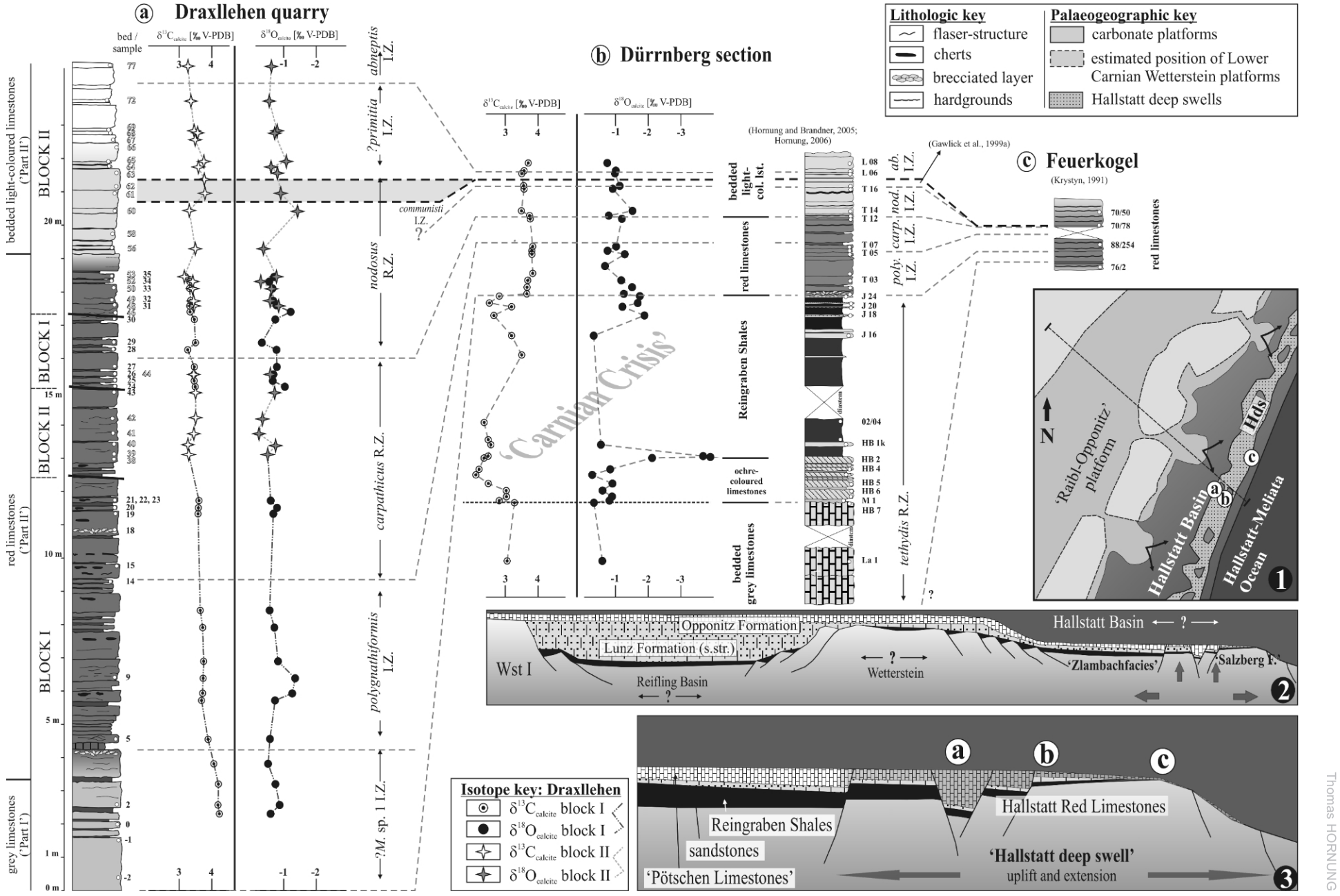

shells. The major proportion on basinal carbonate rocks is periplatform-derived mud – mainly peloidal sands containing comparatively a few siliceous sponge spicules. Short-termed events as storms and/or earthquakes transported the limy mud into basinal areas, where it was re-distributed by bottom-near currents, indicated by interspersed winnowing bioclastic grainstones (Fig. 3e; see also Krystyn, 1991).

Variations in sediment accumulation are indicated by differences in matrix and texture, as well as in the shape of burrows: the fine matrix and homogenous bioturbation in parts I and III points to higher sedimentation rates relatively to part II. Here, grain winnowing, distinct burrowing, micro-bioerosion of lithoclasts and enveloping isopachous cement seams indicate submarine exposure, influence of early marine-phreatic diagenesis and less sediment accumulation. In conclusion, the observed microfacies patterns reflect a relatively quiet depositional environment well below the storm wave base. Here, water depths can be only estimated: whereas Schmidt (1990) argued for 50-100 m, Gawlick and Böhm assumed aphotic water depths of around 300 m.

5.1.2 Hallstatt Limestone sedimentation: the 'Carnian Crisis' and its aftermath

As mentioned shortly above, the 'Carnian Crisis' (Hallam, 1996) was the most incisive Triassic ecologic turnover that lasted from Julian 1/IIc to Julian 2/II (Hornung and Brandner, 2005) and affected mainly reef-builders, benthonic and nektonic organisms (e.g. Simms and Ruffell, 1989; Krystyn, 1991; Hallam, 1996; Rigo et al., 2007), but even terrestric biota (e.g. Benton, 1991). Large amounts of siliciclastic material was swept into intaplatform-basinal troughs (Partnach- and Reifling Basins) and covered even ocean-related environments: ochre-coloured limestones and overlying Reingraben Shales mark the 'Carnian Crisis' in the Hallstatt Basin indicating a Tethyan-wide demise of carbonate platforms and reefs (Hornung and Brandner, 2005; Hornung et al., 2005, 2007 a).

Already in earliest Tuvalian, the pre-existing submarine topography has been changed distinctively: intraplatform-basinal troughs and carbonate platform belts – had been filled up and covered by a lower Lower Carnian mixed siliciclastic-carbonatic sequence ('Northern Alpine Raibl Formation', 'Lunz Formation s.str.'). Where once Wetterstein Carbonate Platforms flourished, dominated by microbial reefs, coral reefs, dasygladacean algae and coralline sponges (Flügel, 2002), a vast shallow-marine peneplain ('Raibl-Opponitz platform', see Figure 5-1) was build mainly by peloidal sands, carbonate precipitated by unknown producers and only minor amounts of reef-building organisms (siliceous sponges: Fig. $3e_3$). Only from the latest Carnian, corals and coralline sponges reappeared and dominated the reef-constructing community again. Typical Lower Carnian microbial algal reefs *(Tubiphytes* sp.), however, had vanished completely (Flügel, 2002).

Deposition of Upper Carnian Hallstatt Limestones was highly influenced by sedimentation in shallow-marine environments (Reijmer and Everaas, 1991). Transgressive stages led to carbonate platform aggradation and low basinal sediment accumulation; sea level highstands caused carbonate platform progradation and high sediment accumulation within the basins ('highstand shedding'-principle of Schlager et al., 1994). This development can be retraced at the Draxllehen succession and is directly linked to the colour of the exposed limestones: Krystyn and Lein (1996) observed a sea level highstand in the Early Tuvalian 1 – increased sedimentation rates led to deposition of grey limestones of 'part I'. Transgressive periods in Tuvalian 1/II-2/II led to low accumulation rates in basins. After the scheme of Bachmann and Jakobshagen (1974), a long-termed exposure of sediments suffered higher oxidation levels over time thus oxidising iron and causing a red to magenta-coloured hue of carbonate rocks. The red colour vanished in Tuvalian 3, when a new sea level highstand led to higher accumulation, less sediment exposure time and, accordingly, lower oxidation levels.

The Tuvalian 3-sea level highstand heralding the development of extended lagoons and reefs on prograding carbonate platforms (Dachstein reefs and lagoonal Hauptdolomite), suffered a short setback, when increased tectonics induced a sea level lowstand (Krystyn and Lein, 1996; Gawlick and Böhm, 2000). At Draxllehen, this is documented by the absence of the Tuvalian 3/II *(communisti* A-Zone) and most probably of the Lacian 1/I *(communisti* B-Zone). Since higher Lacian 1, sediment accumulation increased visibly – by the light-coloured hue of limestones.

5.1.3 Highly varying thicknesses of Hallstatt Red Limestones – new implications of limestone sedimentation upon 'Hallstatt deep swells'

Compared to other biostratigraphically well-controlled (Upper) Carnian sequences (Feuerkogel: Krystyn, 1973, 1978, 1991; Freygutweg: Gawlick et al., 1999; Hornung and Brandner, 2005), which provide thicknesses of only a few metres, the Draxllehen succession reaches comparatively high thicknesses. Although overprinted by flat normal faults, conodont-biostratigraphy allows for a reconstruction of the lithological column, the exclusion of tectonic doubling and/or tripling (as it is assumed for the Tiefenbachgraben succession), and for the cross-correlation highlighted in the Figures 5a-c. Hence, the calibration proofs simultaneity of high condensation (Figs. 5b-c) next to rather 'normal' sedimentary patterns (Fig. 5a).

The explanation for this phenomenon might be seen in locally strongly differing subsidence, caused by extensional movements on an instable passive margin (e.g. Schlager, 1969; Brandner, 1978, 1984). Gradually enforced by synsedimentary halokinetic uplifts, the Upper Permian / Lower Triassic saline 'Haselgebirge' created so-called 'Hallstatt deep swells'. Formerly, these swells were assigned to submarine highs (e.g. Tollmann, 1976, Mandl, 1984, 2000). Present microfacies studies, however, interpret these as an even, least-elevated region at the transition to the oceanic Meliata-Facies (Hornung et al., 2007b; see Figures 5_{1-3}). Both ex-

tensional and halokinetic movements caused local tectonics and synsedimentary fissures (e.g. Schlager, 1969; Hornung, 2005). Listric faults induced block tilting with increased local subsidence. Relative subsidence was low in zones without extension and/or highest uplift rates. Here, bottom currents caused sediment washout being thus responsible for a high-grade condensed facies with abundant Fe-oxide- and manganese-bearing hardgrounds (Feuerkogel section, see Krystyn, 1991; Rappoltstein: see Hornung et al., 2007b). Accordingly, zones affected by extension and/or halokinetic movements (in our case the region around the Draxllehen quarry) formed graben-structures, which absorbed both the periplatform-derived carbonatics detritus and current-transported limy material. Accordingly, the successions exhibit monotonous bedding, absence of hardground and comparatively high thicknesses (Fig. 5_3).

5.2 Stable isotopes

5.2.1 Carbon Isotopes

Isotopic studies of, for instance, Jenkyns et al. (1994), Wortmann and Weissert (2000), and Korte et al. (2005) demonstrated that the $\delta^{13}C_{carb}$ of whole rocks is relatively stable against diagenetic alterations in deep burial stages. Gawlick and Böhm (2000) confirmed this for uppermost Carnian to Upper Norian Hallstatt Limestones from the Kälberstein quarry near Berchtesgaden. From early diagenesis, however, several effects are known that might happen prior and during early recrystallisation. These have been intensively discussed in Gawlick and Böhm (2000) for time-equivalent carbonate rocks in close vicinity of the Draxllehen quarry. Here, the two main possible effects are described shortly:

Marshall (1992) described coupled ^{13}C- and ^{18}O- depletion, in particular, when the primary isotope signal was produced in shallow-marine environment but has been re-equilibrated and stabilized in deeper marine settings. The long-term isotope trend outlined in Figure 5a, however, demonstrates that the $\delta^{13}C_{carb}$ signal show no depletion in ^{13}C when the related ^{18}O-values are lowest (example: horizons D 9, 24, 48, 60).

McCorkle et al. (1985) argued that flow of organic-rich fluids (derived from decay of organic matter) through early carbonate rocks would lower their primary isotopic composition. This potential diagenetic effect can be excluded for the Draxllehen succession, because almost all studied horizons provide the presence of oxidised iron: thus, all organic matter have been oxidised before iron reduction started (Burdige, 1993).

There are only a few studies that reported Late Carnian and Early Norian isotope data (Fig. 6): Korte et al. (2005) and Hornung and Brandner (2005; compare to Figure 5b in this paper) noted a significant rise of carbon isotope values around the Julian / Tuvalian boundary from 1.5 to 4.0 ‰. This shift is followed by high Early Tuvalian values providing a slight declining trend towards the Late Tuvalian (Freygutweg: 3.8 ‰ to 3.3 ‰, see Figure 5b). The same negative trend is visible from the Draxllehen carbon isotopes: high Tuvalian 1 $\delta^{13}C_{carb}$ values of 4.3 ‰ decrease steadily towards Tuvalian 2 (3.7 ‰) and Tuvalian 3 (3.2 ‰).

Gawlick and Böhm (2000) reported a minor positive shift in $\delta^{13}C_{carb}$ from 3.7 to 4.2 ‰ closely above the Carnian-Norian boundary, followed by a slight regressive trend towards lighter $\delta^{13}C_{carb}$ values of 3.5 ‰ in Lacian 2. Hauser et al. (2001) measured a minor C-isotope positive shift of circa 1 ‰ near the FO of *M. communisti*. Muttoni et al. (2004) observed a positive $\delta^{13}C_{carb}$ shift of 1.2 ‰ from the Pizzo Mondello in Sicily (from 1.4 to 2.6 ‰), however, below the FAD of *M.communisti* and 12.5 m below the approximated Carnian-Norian boundary. Present but not yet published isotope investigations of Tuvalian and Lacian limestones of Slovakia (Silická Brezova) and Turkey (Bölücektasi Tepe and Erenkolu Mezarlik) observed a similar, minor positive $\delta^{13}C_{carb}$-shift of 0.5 ‰ in the lower part of the *communisti* B interval zone (lower *kerri* Zone or Lacian 1/l; S. Richoz, pers. comm. 2007). At Draxllehen,

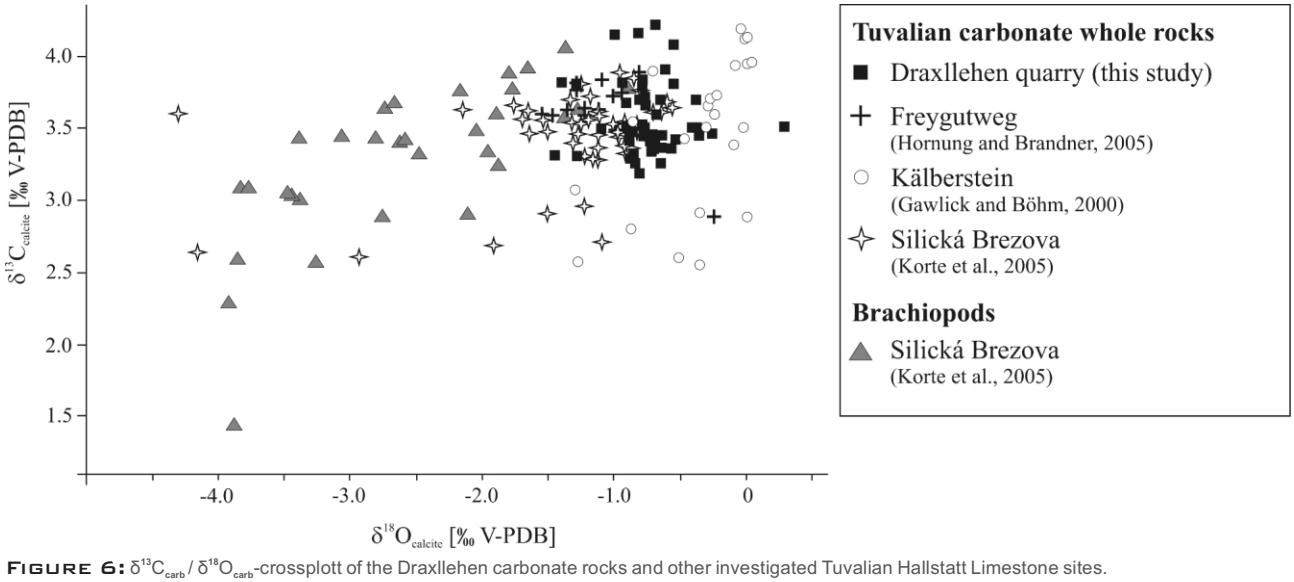

Figure 6: $\delta^{13}C_{carb}$ / $\delta^{18}O_{carb}$-crossplott of the Draxllehen carbonate rocks and other investigated Tuvalian Hallstatt Limestone sites.

too, a minor positive shift of 0.4 ‰ is observed between D 60 and D 61, i.e. within the Carnian-Norian boundary interval. In comparison, the carbon isotope trend of the adjacent Freygutweg shows no positive shift at this level, maybe due to the very high condensation rate (Hornung and Brandner, 2005).

In conclusion, the above short review of Late Carnian / Early Norian isotope values in comparison to the new Draxllehen data provide a Tuvalian regressive trend, followed by a shift towards more positive values around the Carnian-Norian boundary. However, as the excursions range within an amplitude that may derive from regional and lithological variations (S. Richoz, pers. comm. 2007), the Carnian-Norian carbon isotope shifts may suggest not an isotopic boundary markerevent of global importance as proposed by Gawlick and Böhm (2000). Additionally to well-established biostratigraphy, this could be used to correlate high-resolution C-isotope curves of boundary sections.

5.2.2 Oxygen isotopes

The stable average value of $\delta^{18}O_{carb}$ centred around -0.3 to -0.5 ‰, no measurable amounts of dolomite, and a CAI of 1.0 are strong indications that the Hallstatt Red Limestones of the Draxllehen quarry have suffered only little diagenetic overprinting. Unlike to carbon, the oxygen isotope signal is relatively sensitive against alteration in shallow burial, as it may be re-equilibrated when the carbonate mud was dislocated to other settings (discussed in Gawlick and Böhm, 2000, cum lit.). As outlined above, nearly all Tuvalian carbonate mud derived from the shallow-marine carbonate platforms and was transported afterwards at distal periplatform settings. The oxygen isotope signal re-equilibrated at greater water depths and colder temperatures and was thus shifted towards higher values. Following Korte et al. (2005), the $\delta^{18}O_{carb}$ ratio of whole rocks is an unsatisfactory tool in reconstructing seawater temperatures.

Gawlick and Böhm (2000) emitted $\delta^{18}O_{carb}$ Hallstatt Limestone-values lower than -0.5 ‰ from their interpretations assigning them as diagenetially altered. However, calculating with ice-free Triassic seawater near a potential scatter from -1 ‰ to -0.25 [V-SMOW] for subtropical environments (Shackleton and Kennett, 1975; Zachos et al., 1994), a $\delta^{18}O_{carb}$ value of 0 ‰ would result in water temperatures ranging between 11 and 14°C (after O'Neil et al., 1994) what equates water depths of more than 500 m (after the World Ocean Data Center: http://www.nodc.noaa.gov/OC5/indprod.html), significantly deeper as previously assumed for the Hallstatt Basin (e.g. Zankl, 1971; Rieche, 1971; Reading, 1986; Schmidt, 1990). Owing to the above reasons, interpretation of this discrepancy might be due to diagenesis and not record primary depositional conditions. Calculation of seawater temperatures and thus palaeobathymetric reconstructions can be better achieved in using brachiopods or aragonite shells (Korte et al., 2005) or measuring the $\delta^{18}O_{phos}$ trend of conodont apatite (e.g. Joachimski et al., 2006; Hornung, 2007; Hornung et al., 2007a, c).

6. Conclusions

1) The Draxllehen quarry allows the rare chance to study a nearly complete and expanded Upper Carnian to Lower Norian Hallstatt Limestone succession that reflects distal periplatform depositional environment and, controlled by low CAI values, suffered only a mild diagenetic alteration.
2) The studied succession differs significantly from yet established Tuvalian and Lacian successions by its monotonous bedding, comparatively high thicknesses and consistent sedimentation. This infers low but rapidly revived carbonate precipitation in the direct aftermath of the 'Carnian carbonate productivity crisis'.
3) Biostratigraphically well-controlled comparisons to adjacent sites exhibit high variations of absolute thicknesses of Hallstatt Red Limestones and confirm the highly variable, tectonically triggered sedimentary patterns on 'Hallstatt deep swells'.
4) Owing to its mild diagenetic alteration, the Draxllehen site was suitable for carbon and oxygen whole rock isotope stratigraphy. Existing data point to varying and comparison with locally depending $\delta^{13}C_{carb}$ trends rather than a supraregional or even global isotopic signal.

Acknowledgements

Thanks are due to Rainer Brandner (Innsbruck) for discussion and providing of lithostratigraphic data as well as thin sections, Antonio Donato Donofrio (Innsbruck) and Manuel Rigo (Padua) for discussions concerning conodont taxonomy. The analytical supports of Christoph Spötl (whole rock isotopy) and Richard Tessadri (XRD-Analysis, both Innsbruck) are highly appreciated. The reviews of Manuel Rigo (Padua), Anonymus and Leo Krystyn (Vienna) helped substantially to improve this paper. This study was supported by the Austrian Science Fund (FWF) in the framework of the project P 16878-N10 GEO (Rainer Brandner).

References

Bachmann, G.H. and Jacobshagen, V., 1974. Zur Fazies und Entstehung der Hallstätter Kalke von Epidauros (Anis bis Karn; Argolis, Griechenland). Zeitschrift der Deutschen Geologischen Gesellschaft, 125, 195-223.

Bralower, T.J., Bown P.R. and Siesser, W.G., 1992. Significance of Upper Triassic nannofossils from the Southern Hemisphere (ODP Leg 122, Wombat Plateau, N.W. Australia). Marine Micropalaeontology, 17, 119-154.

Bellanca, A., Di Stefano, P. and Neri, R., 1995. Sedimentology and isotope geochemistry of Carnian deep-water marl/limestone deposits from the Sicani Mountains, Sicily: Environmental implications and evidence for planktonic source of lime mud. Palaeogeography Palaeoclimatology, Palaeoecology, 114, 111-129.

Benton, M.J., 1991. What really happened in the Late Triassic? Historical Biology, 5, 263-278.

Bhargava, O.N., Krystyn, L., Balini, M., Lein, R. and Nicora, A., 2004. Revised Litho- and Sequence Stratigraphy of the Spiti Triassic. Albertiana, 30, 21-39.

Brandner, R., 1978. Tektonisch kontrollierter Sedimentationsablauf im Ladin und Unterkarn der westlichen Nördlichen Kalkalpen. Geologisch-Paläontologische Mitteilungen Innsbruck, 8, 317-354.

Brandner, R., 1984. Meeresspiegelschwankungen und Tektonik in der Trias der NW-Tethys. Jahrbuch der Geologischen Bundesanstalt, 126 (45), 435-475.

Budurov, K., 1972. *Ancryogondolella triangularis* gen. et sp. n. (Conodonta). Mitteilungen der Gesellschaft geologischer Bergbaustudenten, 21, 855-859.

Burdige, D.J., 1993. The biogeochemistry of manganese and iron reduction in marine sediments. Earth Science Reviews 35, 249-284.

Channel, J.E.T. and Kozur, H.W., 1997. How many oceans? Meliata, Vardar, and Pindos oceans in Mesozoic Alpine Paleogeography. Geology, 25, 183-186.

Channell, J.E.T., Kozur, H.W., Sievers, T., Mock, R.; Aubrecht, R. and Sykora, M., 2003. Carnian-Norian biomagnetostratigraphy at Silicka Brezova (Slovakia): correlation to other Tethyan sections and to the Newark Basin. Palaeogeography, Palaeoclimatology, Palaeoecology, 191, 65-109.

Decker, K., Faupl, P. and Müller A., 1987. Synorogenic sedimentation on the Northern Calcareous Alps during the Early Cretaceous. In: H.W. Flügel and P. Faupl (eds.), Geodynamics of the Eastern Alps (Deutike), 126-141.

Donofrio, D.A., 1975. Mikrofaunistische Untersuchungen der Hallstätter Kalke in den Berchtesgadener Alpen. Unpublished Dissertation University of Innsbruck, 162 pp.

Epstein, A.G., Epstein, J.B., and Harris, L.D., 1977. Conodont colour alteration an index to organic metamorphism. U.S. Geological Survey Professional Paper, 995, 27.

Flügel, E., 2002. Triassic reef patterns. In: W. Kiessling, E. Flügel, J. and Golonka, (eds.), Phanerozoic Reef Patterns. SEPM Special Publication, 72, 391-463.

Frank, W., 1987. Evolution of the Austroalpine Elements in the Cretaceous. In: H.W. Flügel and P. Faupl (eds.), Geodynamics of the Eastern Alps, Deutike, 379-406.

Frisch, W. and Gawlick, H.-J., 2003. The nappe structure of the central Northern Calcareous Alps and its disintegration during Miocene tectonic extrusion – a contribution to understanding the orogenic evolution of the Eastern Alps. International Journal of Earth Sciences, 92, 712-727.

Gallet, Y., Besse, J., Krystyn, L., Théveniaut, H. and Marcoux, J., 1994. Magnetostratigraphy of the Mayerling section (Austria) and Erenkolu Mezarlik (Turkey) section: Improvement of the Carnian (Late Triassic) magnetic polarity time scale. Earth Planetary Science Letters, 125, 173-191.

Gallet, Y., Besse, J., Krystyn, L. and Marcoux, J., 1996. Norian magnetostratigraphy of the Scheiblkogel section Austria: constraint on the origin of the Antalya Nappes, Turkey. Earth Planetary Science Letters, 140, 113-122.

Gallet, Y., Krystyn, L., Besse, J. and Marcoux, J., 2003. Improving the Upper Triassic numerical time scale from cross-correlation between Tethyan marine sections and the continental Newark basin sequence. Earth Planetary Science Letters, 212, 255-261.

Garzanti, E., Jadoul, F., Nicora, A. and Berra, F., 1995. Triassic of Spiti (Tethys Himalaya, N India). Rivista Italiana di Paleontologia e Stratigrafia, 101 (3), 267-300.

Gawlick, H.-J., 1993. Triassische Tiefwasserkomponenten (Kieselkalke, Radiolarite) in der jurassischen Strubbergbrekzie am Tennengebirgsnordrand (Nördliche Kalkalpen, Österreich). Jahrbuch der Geologischen Bundesanstalt, 136, 347-350.

Gawlick, H.-J., 2000. Paläogeographie der Obertrias-Karbonatplattformen in den Nördlichen Kalkalpen. Exkursionsführer Sediment 2000. Mitteilungen der Gesellschaft der Geologie- und Bergbaustudenten Österreichs, 44, 46-95.

Gawlick, H.-J. and Königshof, P., 1993. Diagenese, niedrig- und mittelgradige Metamorphose in den südlichen Salzburger Kalkalpen – Paläotemperatur-Abschätzung auf der Grundlage von Conodont-Colour-Alteration-Index-(CAI-) Daten. Jahrbuch der Geologischen Bundesanstalt, 136(1), 39-48.

Gawlick, H.-J., Lein, R. and Krystyn, L., 1994. Conodont colour alteration indices: Palaeotemperatures and metamorphism in the Northern Calcareous Alps – a general view. Geologische Rundschau, 83, 660 – 664.

Gawlick, H.-J. and Lein, R., 1997. Neue stratigraphische und fazielle Daten aus dem Jakobberg- und Wolfdietrichstollen des Hallein- Bad Dürrnberger Salzberges und ihre Bedeutung für die Interpretation der geologischen Verhältnisse im Bereich der Hallein-Berchtesgadener Schollenregion. Geologisch-Paläontologische Mitteilungen Innsbruck, 22, 199-225.

Gawlick, H.-J., Lein, R., Piros, O. and Pytel C., 1999. Zur Stratigraphie und Tektonik des Hallein – Bad Dürrnberger Salzberges – Neuergebnisse auf der Basis von stratigraphischen und faziellen Daten (Nördliche Kalkalpen, Salzburg). Abhandlungen der Geologischen Bundesanstalt, 56/2, 69-90.

Gawlick, H.-J. and Böhm, F., 2000. Sequence and isotope stratigraphy of Late Triassic distal periplatform-limestones from the Northern Calcareous Alps (Kälberstein Quarry, Berchtesgaden Hallstatt Zone). Geologische Rundschau, 89, 108-129.

Gawlick, H.-J. and Lein, R., 2000. Die Salzlagerstätte Hallein – Bad Dürrnberg. Exkursionsführer Sediment 2000, Mitteilungen der Gesellschaft der Geologie- und Bergbaustudenten Österreichs, 44, 263-280.

Gawlick, H.-J-, Suzuki, H. and Missoni, S. 2001. Nachweis von unterliassischen Beckensedimenten in Hallstätter Fazies (Dürrnberg-Formation) im Bereich der Hallein-Berchtesgadener Hallstätter Zone und des Lammer Beckens (Hettangium-Sinemurium). Mitteilungen der Gesellschaft der Geologie- und Bergbaustudenten Österreichs, 45, 39-55.

Gümbel, C.W., 1861. Geognostische Beschreibung des Bayrischen Alpengebirges und seines Vorlandes. Perthes-Verlag, Gotha, 940 pp.

Haas, J., Kovács, S., Krystyn, L. and Lein, R., 1995. Significance of Late Permian-Triassic facies zones in terrane reconstructions in the Alpine-North Pannonian domain. Tectonophysics, 242, 19-40.

Hallam, A., 1996. Major Bio-Events in the Triassic and Jurassic. In: Walliser, O.H (Ed.): Global Events and Event-Stratigraphy, Springer, 332 pp.

Hauser, M., Martini, R., Burns, S., Dumitrica, P., Krystyn, L., Matter, A., Peters, T. and Zaninetti, L., 2001. Triassic evolution of the Arabian-Greater India embayment of the southern Tethys margin. Eclogae geologica Helveticae, 94, 29-62.

Hayashi, S., 1968. The Permian conodonts in chert of the Adoyama Formation, Ashio Mountains, Central Japan. Earth Science, 22, 63-77.

Hornung, T., 2005. Palaeoclimate background and stratigraphic evidence of Late Norian / early Rhaetian polyphase synsedimentary tectonics in the Hallstatt Limestones of Berchtesgaden (Rappoltstein, Southern Germany). Austrian Journal of Earth Sciences, 98, 106-119.

Hornung, T., 2006a. Das Karnische Ereignis der Halleiner Salzberg-Fazies (distale Hallstatt-Fazies): biostratigraphische Daten. Geo.Alp, 3, 9-21.

Hornung, T., 2006b. Conodont biostratigraphy of the Lercheck / Königsleiten section near Berchtesgaden (Late Ladinian – Hallstatt Limestones). Geo.Alp, 3, 23-31.

Hornung, T. and Brandner, R., 2005. Biochronostratigraphy of the Reingraben Turnover (Hallstatt Facies Belt): Local black shale events controlled by regional tectonics, climatic change and plate tectonics. Facies, 51, 460-479, DOI: 10.1007/s10347-005-0061-x.

Hornung, T., Brandner, R. and Krystyn, L., 2005. Carnian black shale events triggered by Cimmerian-Eurasian collision? Abstract Book / CD, EGU-Meeting April 2005, Vienna.

Hornung, T., 2007. The 'Carnian Crisis' in the Tethys realm: multistratigraphic studies and palaeoclimate constraints. PhD-Thesis University of Innsbruck, 233 pp + VII, 1 CD-Rom.

Hornung, T., Krystyn, L. and Brandner, R., 2007a. A Tethys-wide mid-Carnian (Upper Triassic) carbonate productivity decline: Evidence for the Alpine Reingraben Event from Spiti (Indian Himalaya)? Journal of Asian Earth Sciences, 30, 285-302; doi: 10.1016/j.jseaes.2006.10.001.

Hornung, T., Spatzenegger, A. and Joachimski, M.M., 2007b. Multistratigraphy of condensed ammonoid beds of the Rappoltstein (Berchtesgaden, Southern Germany): unravelling palaeoenvironmental conditions on 'Hallstatt deep swells' during the Reingraben Event (late Lower Carnian). Facies, 53, 267-292, doi: 10.1007/s10347-006-0101-1.

Hornung, T., Brandner, R., Krystyn, L., Joachimski, M.M., and Keim, L., 2007c. Multistratigraphic constraints on the NW Tethyan 'Carnin Crisis' - In: Lucas, S.G., Spielmann, J.A. (Eds.): The Global Triassic. New Mexico Museum of Natural History Bulletin, 41, 59-67.

Huckriede, R., 1958. Die Conodonten der mediterranen Trias und ihr stratigraphischer Wert. Paläontologische Zeitschrift, 32/3-4, 141-175.

Janofske, D., 1992. Kalkiges Nannoplankton, insbesondere kalkige Dinoflagellaten-Zysten der alpinen O.-Trias: Taxonomie, Biostratigraphie und Bedeutung für die Phylogenie der Peridinales. Berliner Geowissenschftliche Abhandlungen, E 4, 1-53.

Jenkyns, H.C., Gale, A.S. and Corfield, R.M., 1994. Carbon- and oxygen-isotope stratigraphy of the English Chalk and Italian Scaglia and its palaeoclimatic significance. Geological Magazine, 131, 1-34.

Joachimski, M.M., v. Bitter, B.H. and Buggisch, W., 2006. Constraints on Pennsylvanian glacioeustatic sea-level changes using oxygen isotopes of conodont apatite. Geology, 34/4, 277-280.

Jones, G.L., 1992. Irish Carboniferous conodonts record maturation levels and the influence of tectonism, igneous activity and mineralization. Terra Nova, 4, 238-244.

Kolar-Jurkovsek, T., 1983. Srednjetriasni konodonti Slovenije. Rud.-met. Zbor. 30/4, 323-364.

Korte, C., Kozur, H.W. and Veizer, J., 2005. $\delta^{13}C$ and $\delta^{18}O$ values of Triassic brachiopods and carbonate rocks as proxies for coeval seawater and palaeotemperature. Palaeogeography, Palaeoclimatology, Palaeoecology, 226, 287-306.

Kovács, S., 1983. On the evolution of *excelsa*-stock in the Upper Ladinian-Carnian (Conodonta, genus *Gondolella*, Triassic). Schriftenreihe der Erdwissenschaftlichen Kommission Österreichisch-Akademischer Wissenschaften, 5, 107-119.

Kovács, S. and Kozur, H., 1980. Stratigraphische Reichweite der wichtigsten Conodonten (ohne Zahnreihen-Conodonten) der Mittel- und Obertrias. Geologisch-Paläontologische Mitteilungen Innsbruck, 10/2, 42-78.

Kozur, H., 1972. Die Conodontengattung *Metapolygnathus* Hayashi 1968 und ihr stratigraphischer Wert. Geologisch-Paläontologische Mitteilungen Innsbruck, 2 (11), 1-37.

Kozur, H., 2003. Integrated ammonoid, conodont and radiolarian zonation of the Triassic and some remarks to Stage/Substage subdivision and the numeric age of the Triassic stages. Albertiana, 28: 57-74.

Kozur, H. and Mostler, H., 1992. Erster paläontologischer Nachweis von Meliaticum und Süd-Rudabányaicum in den Nördlichen Kalkalpen (Österr.) und ihre Beziehungen zu den Abfolgen in den Westkarpaten. Geologisch-Paläontologische Mitteilungen Innsbruck, 18, 87-129.

Krystyn, L., 1973. Zur Ammoniten- und Conodonten-Stratigraphie der Hallstätter Obertrias (Salzkammergut, Österreich). Verhandlungen der Geologischen Bundesanstalt, 1973/1, 112-153.

Krystyn, L., 1978. Eine neue Zonengliederung im alpin-mediterranen Unterkarn. Schriftenreihe der Erdwissenschaftlichen Kommission Österreichischer Akademischer Wissenschaften, 4: 37-75.

Krystyn, L., 1980. Triassic conodont localities of the Salzkammergut Region (Northern Calcareous Alps). In: Second European Conodont Symposium-ECOS II, Guidebook and Abstracts. Abhandlungen der Geologischen Bundesanstalt, 35, 61-98.

Krystyn, L., 1983. The Epidauros Section (Greece) – a contribution to the conodont standard zonation of the Ladinian and Lower Carnian of the Tethys Realm. Schriftenreihe der Erdwissenschaftlichen Kommission der Österreichischen Akademie der Wissenschaften, 5, 231-258.

Krystyn, L., 1991. Die Fossillagerstätten der alpinen Trias. Exkursionsführer, Wien.

Krystyn, L. and Lein, R. 1996. Triassische Becken- und Plattformsedimente der östlichen Kalkalpen. In: Exkursionsführer 11. Sedimentologentreffen Wien, Berichte der Geologischen Bundesanstalt Wien, 33, 23 pp.

Krystyn, L. and Gallet, Y., 2002. Towards a Tethyan Carnian-Norian boundary GSSP. Albertiana, 8, 15-24.

Krystyn, L., Gallet, Y., Besse, J. and Marcoux, J. 2002. Integrated Upper Carnian to Lower Norian biochronology and implications for the Upper Triassic magnetic polarity time scale. Earth Planetary Science Letters, 203, 343-351.

Langenscheidt, E., 1994. Geologie der Berchtesgadener Berge. Nationalparkverwaltung Berchtesgaden, Berchtesgaden, 1-155.

Lehrmann, D.J., Enos, P., Payne, J.L., Montgomery, P., Wei, J., Yu, Y., Xiao, J., and Orchard, M., 2005. Permian and Triassic depositional history of the Yangtze platform and Great Bank of Guizhou in the Nanpanjiang Basin of Guizhou and Guangxi, south China. Albertiana, 33, 149-168.

Lintnerova, O. and Hladikova, J., 1992. Distribution of stable O and C isotopes and microelements in Triassic limestones of the Veterlín unit, the Malé Karpaty Mts.: their diagenetic interpretation. Geologica Carpathica, 43, 203-212.

Mandl, G.W., 1984. Zur Trias des Hallstätter Raumes – ein Modell am Beispiel Salzkammergut (NKA, Österreich). Mitteilungen der Gesellschaft der Geologie- und Bergbaustudenten Österreichs, 30/31: 133-176.

Mandl, G.W., 2000. The Alpine sector of the Tethyan Shelf – Examples of Triassic to Jurassic sedimentation and deformation from the Northern Calcareous Alps. Mitteilungen der Österreichischen Geologischen Gesellschaft, 92, 61-79.

Mandl, G.W., and Ondrejickova, A., 1993. Radiolarien und Conodonten aus dem Meliatikum im Ostabschnitt der Nördlichen Kalkalpen (Österreich). Jahrbuch der Geologischen Bundesanstalt, 136, 841-876.

Marshall, J.D., 1992. Climatic and oceanographic isotopic signals from the carbonate rock record and their preservation. Geological Magazine, 129 (2), 143-160.

Martini, R., Zaninetti, L., Villeneuve, M., Corné, J.-J., Krystyn, L., Cirilli, S., De Wever, P., Dumitrica, P. and Harsolumakso, A., 2000. Triassic pelagic deposits of Timor: palaeogeographic and sea-level implications. Palaeogeography, Palaeoclimatology, Palaeoecology, 160, 123-151.

McCorkle, D.C., Emerson, S.R. and Quay, P.D., 1985. Stable isotopes in marine porewaters. Earth and Planetary Science Letters, 74, 13-26.

Missoni, S., 2003. Analyse der mittel- und oberjurassischen Beckenentwicklung in den Berchtesgadener Kalkalpen – Stratigraphie, Fazies und Paläogeographie. Unpublished PhD Thesis, Montan-University Leoben, 1–150.

Mock, R., 1979. *Gondolella carpathica* n. sp., eine wichtige tuvalische Conodontenart. Geologisch-Paläontologische Mitteilungen Innsbruck, 9 (4), 171-174.

Muttoni, G., Kent, D.V., Olsen, P.E., di Stefano, P., Lowrie, W., Bernasconi, S.M. and Hernández, F.M., 2004. Tethyan magnetostratigraphy from Pizzo Mondello (Sicily) and correlation to the late Triassic Newark astrochronological polarity time scale. GSA Bulletin, 116 (9/10), 1043-1058.

O'Neil J.R., Roe L.J., Reinhard E. and Blake R.E., 1994. A rapid and precise method of oxygen isotope analysis of biogenic phosphate. Israel Journal of Earth Science, 43 (3-4), 203-212.

Orchard, M.J., 1983. *Epigondolella* populations and their phylogeny and zonation in the Upper Triassic. Fossils and Strata, 15, 177-192.

Orchard, M.J., 1991a. Late Triassic conodont biochronology and biostratigraphy of the Kunga Group, Queen Charlotte Islands, British Columbia. In: Woodsworth, G.J. (ed.): Evolution and Hydrocarbon Potential of the Queen Charlotte Basin, British Columbia. Geological Survey of Canada, 90(10), 173-193.

Orchard, M.J., 1991b. Upper Triassic conodont biochronology and new index species from the Canadian Cordillera. In: Orchard, M.J., McCracken (eds.): Ordovician to Triassic Conodont Paleontology of the Canadian Cordillera. Geological Survey of Canada, Bulletin, 417, 299-335.

Pichler, H., 1963. Geologische Untersuchungen im Gebiet zwischen Rossfeld und Markt Schellenberg im Berchtesgadener Land. Beihefte des Geologischen Jahrbuches, 48, 129-204.

Plöchinger, B., 1955. Zur Geologie des Kalkalpenabschnittes vom Torrener Joch zum Ostfuß des Untersberges; die Göllmasse und die Halleiner Hallstätter Zone. Jahrbuch der Geologischen Bundesanstalt., 95/1, 93-144.

Reading, H., 1986. Sedimentary environments and facies. 2nd Edition, Oxford (Blackwell), 615 pp.

Reijmer, J.J.G. and Everaas, S.L., 1991. Carbonate platform facies reflected in carbonate basin facies (Triassic, Northern Calcareous Alps, Austria). Facies, 25, 253-278.

Rieche, J. 1971. Die Hallstätter Kalke der Berchtesgadener Alpen. Unpublished PhD Thesis TU Berlin, 173 pp.

Rigo, M., Preto, N., Roghi, G., Tateo, F. and Mietto, P., 2007. A rise in the carbonate Compensation Depth of western Tethys in the Carnian (Late Triassic): Deep-water evidence for the Carnian Pluvial Event. Paleogeography, Paleoclimatology, Palaeoecology, 246 (2-4), 188-205.

Schafhäutl, K. E. v., 1851. Geognostische Untersuchungen des südbayrischen Alpengebirges. München, 206 pp.

Schlager, W., 1969. Das Zusammenwirken von Sedimentation und Bruchtektonik in den triadischen Hallstätterkalken der Ostalpen. Geologische Rundschau, 59, 289-308.

Schlager, W., Reijmer, JJG. and Droxler, A., 1994. Highstand shedding of carbonate platforms. Journal of Sedimentary Research, B 64, 270-281.

Schlosser, M., 1898. Das Triasgebiet von Hallein. Zeitschrift der deutschen Geologischen Gesellschaft, 50, 333-384.

Schmidt, H., 1990. Mikrobohrspuren in Fossilien der triassischen Hallstätter Kalke und ihre bathymetrische Bedeutung. Facies, 23, 109-120.

Shackleton, N.J. and Kennett, J.P., 1975. Late Cenozoic oxygen and carbon isotopic changes at DSDP Site 284; implications for glacial history of the Northern Hemisphere and Antarctica. Initial Reports of the Deep Sea Drilling Project, 29, 801-807.

Simms M.J. and Ruffell A.H., 1989. Synchroneity of climate change and extinctions in the Late Triassic. Geology 17, 265-268.

Spötl, C. and Vennemann, T.W., 2003. Continuous-flow isotope ratio mass spectrometer analysis of carbonate minerals. Rapid Communication Mass Spectrometry, 17, 1004-1006.

Steuber, T., 1989. Conodonten, Mikrofazies und Isotopengeochemie der Trias im Helikon-Gebirge, Griechenland. Sonderveröffentlichungen des Geologischen Instituts der Universität Köln, 73, 1-94.

Tollmann, A., 1976. Analyse des klassischen nordalpinen Mesozoikums: Stratigraphie, Fauna und Fazies der Nördlichen Kalkalpen XV, 580 pp., Wien.

Tollmann, A., 1985. Geologie von Österreich. Vol.2, Deuticke, 710 pp., Wien.

Wortmann, U.G. and Weissert, H. 2000. Tying platform drowning to perturbations of the global carbon cycle with a $\delta^{13}C_{org}$-curve from the Valanginian of DSDP Site 416. Terra Nova, 12, 289-294.

Zachos, J.C., Scott, L.D., and Lohmann, K.C., 1994. Evolution of early Cenozoic marine temperatures. Paleoceanography, 9, 353–387.

Zankl, H., 1971. Upper Triassic carbonate facies in the northern Limestone Alps. In: Müller, G., and Friedman G. (Eds): Sedimentology of parts of Central Europe. Kramer, Frankfurt, 147-185.

Received:10. February 2007
Accepted: 08. August 2007

Thomas HORNUNG

University of Innsbruck, Institute of Geology & Palaeontology, Innrain 52, 6020 Innsbruck, Austria. e-mail: tompal@gmx.net

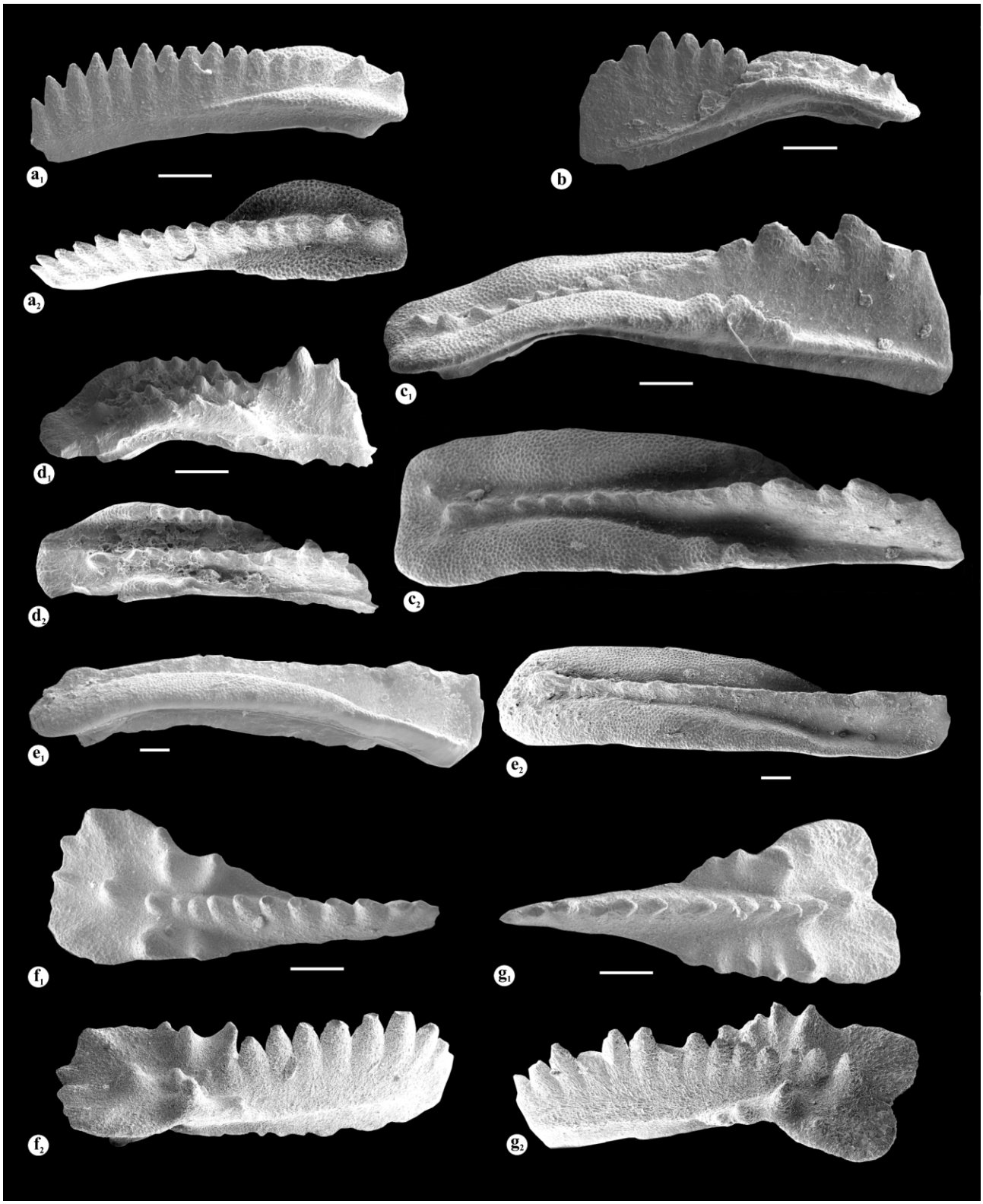

Plate 1:

Conodonts of the Draxllehen section

Figure a: *Metapolygnathus tadpole* (Hayashi, 1968); a_1) angular view; a_2) upper view; (D -2),

Figure b: *Metapolygnathus polygnathiformis* (Stefanov and Budurov, 1965); angular view; (D 39),

Figure c: *Metapolygnathus carpathicus* (Mock, 1979); c_1) angular view; c_2) lateral view; (D 14),

Figure d: *Metapolygnathus nodosus*; posteriorly broken specimen d_1) lateral view; d_2) upper view; (D 53),

Figure e: *Norigondolella navicula* (Huckriede, 1958); e_1) lateral view; e_2) upper view; (D 68),

Figure f: *Epigondolella triangularis* n. subsp. (sensu Krystyn and Gallet, 2002); f_1) upper view; f_2) angular view; (D 77),

Figure g: *Epigondolella triangularis* n. subsp. (sensu Krystyn and Gallet, 2002); g_1) upper view; g_2) angular view; (D 77)